Journal of Applied Mechanics Vol. 6, pp. 1097-1104 (August 2003) JSCE

Inverse Analysis to Determine Crack Bridging Stress in Fiber Composites

繊維補強複合材料におけるひび割れ架橋応力の逆解析

Mohammad Nazmul Islam* and Takashi Matsumoto**

イスラム モハマド ナズムル・松本高志

*Graduate student, Dept. of Civil Eng., Univ. of Tokyo (7-3-1, Hongo, Bunkyo-ku, Tokyo 113-8656)
**Ph.D., Assoc. Prof., Dept. Civil Eng., Univ. of Tokyo (7-3-1, Hongo, Bunkyo-ku, Tokyo 113-8656)

This paper develops a method to determine "bridging law" for continuously aligned fiber composites to understand damage mechanisms from a maintenance engineering point of view. Fracture mechanics approach has been employed to form the integral equation for mathematical simulation of embedded straight cracks and single edge cracks in specimens of infinite or finite width under tensile and bending stresses. Closing pressure was assumed between the crack surfaces due to continuous fibers or aggregates which remain connected to both the crack surfaces. Inverse analysis is performed on crack opening displacement (COD) data to get magnitude and distribution of bridging stresses for fiber composites. Synthetic data were created by forward analysis for certain crack configurations to get exact COD data from a theoretical point of view. To simulate practical situations, data were made noisy by inserting noise of known levels. Exact bridging stress distributions were retrieved by the inverse analysis up to certain level of noisy data which establishes applicability of the method developed here.

Key Words: *fiber composites, fracture mechanics, crack opening displacement, inverse analysis, crack bridging stress.*

1. Introduction

Fiber composites have got extensive role in maintenance engineering in recent years for repair and retrofit in concrete structures. Determination of capacity of those materials at service is an important task to assess sustainability and durability of maintenance work. Traditionally, non-destructive testing and evaluation (NDT&E) methods have been employed for this purpose where the techniques incorporate their own disadvantages and/or limitations. This paper focuses on that issue from a different point of view. Mechanics of fiber composites is studied here with a view to determine the "bridging law" for composites where ductile fibers are continuously aligned in a brittle matrix. While estimating necessity and designing the extent of maintenance work, such bridging law helps engineers to analyze the structure by fracture mechanics.

Tensile capacity of low strength brittle materials can be greatly improved with high strength ductile fiber inclusion into the brittle matrix. These types of composites can sustain large strains before failure with cracks developed in the matrix while the fibers remain intact supplying sufficient closing pressures and arresting crack propagation. Bridging stresses between the crack surfaces develop from continuous fibers or individual grains which remain connected with both the crack surfaces after the crack has been propagated for a sufficient distance from an initial notch or due to indentation. If the dimensions of those fibers/grains are small enough compared with the crack geometry, bridging stresses can be considered as a uniform closing pressure between the crack surfaces. These bridging tractions can be expressed mathematically as a function of distance along the crack for most of the brittle-matrix composites. Under monotonic loading, bridging tractions can also be expressed as a function of COD. In fatigue analysis, bridging stresses can be expressed with COD if appropriate mathematical modeling is done for the processes involved e.g. interfacial debonding, interfacial sliding, matrix microcracking and plastic deformations.

Ductile inclusion into brittle matrix can be done either by distributing fibers randomly in the matrix forming discontinuous fiber reinforced composites (DFRC) or by continuously aligning (CA) the fibers in a row; each method leading to different bridging laws. Detailed theoretical prediction and design model for DFRC's are available in [1] where mechanics of CA brittle-matrix composites can be found in [2-5]. Similar approach (a stepped inverse analysis) was adopted in [8] where a poly-linear tension softening diagram was analyzed on the cohesive force model to determine fracture parameters of plain concrete. This paper addresses to CA brittle-matrix composites with the mechanics derived from [2] and [3]. Inverse analysis is performed here to determine crack bridging stresses from the COD data. Susceptibility of COD data to different noise levels was tested and it is recommended to reduce noise level as much as possible to get better results.

Two types of specimens of brittle matrix composites have been considered in this paper e.g. embedded straight crack specimen (centrally cracked) and single edge cracked specimen. Analyses were performed firstly for infinite width of these specimens under remotely applied uniform tensile stresses. Secondly, single edge cracked specimens under bending stresses are analyzed for finite width to prove the applicability of the model for bending analysis as well. Other crack specimens (double edge crack, compact tension specimens etc.) can also be analyzed similarly with this method. During the solution process, it is assumed that bridging is the only active toughening mechanism and the other sources e.g. stress-strain hysteresis due to microcracking ahead of the crack tip and effect of T-stresses are neglected.

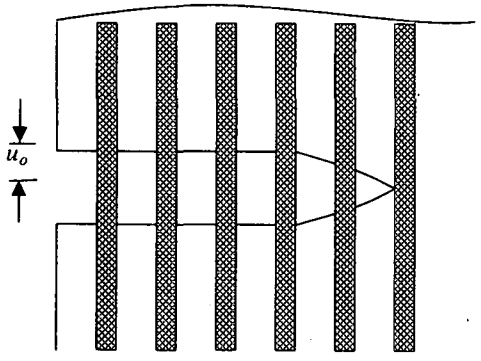

Fig. 1a: Schematic representation of a CA brittle-matrix composite

Bridging stresses in CA brittle-matrix composites can be simulated considering elongation of fiber against its elastic strength and fiber pull-out against friction between fiber- matrix interfaces (chemical bond between matrix and fiber has been neglected here). This can be started with a single-fiber pull-out analysis. It was shown in [4] that the applied stress in a single fiber pull-out test is proportional to the square-root of the fiber pull-out length which can be depicted as in Fig. 1b, where Fig. 1a shows a cracked CA brittle-matrix composite where fibers are bridging crack extension

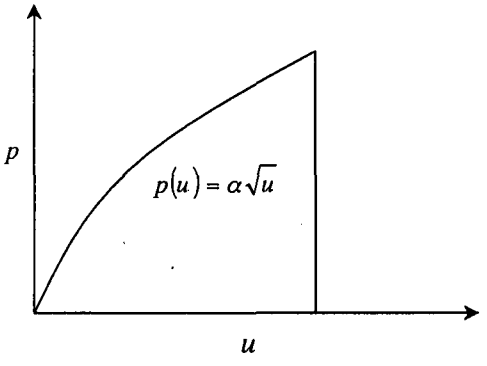

Fig. 1b: Single fiber pull-out stress (p) vs. pull-out distance (u).

However, two main regions of behavior have been identified for CA brittle-matrix composites in which bridging stresses are determined by frictional sliding between the fibers and the matrix and the fibers possess a single valued strength. Firstly, fibers are sufficiently strong and continue to bridge the matrix cracks even when it extends completely through the matrix leading to multiple matrix cracking and non-catastrophic failure. This situation is called fully bridged cracks and they continue to bridge the cracks until the fiber ultimate strength is reached. Secondly, if the fibers are not that much strong compared to the applied load, they break in the crack-wake leaving only a small portion of bridged zone just behind the crack tip. This leads to catastrophic failure, although bridging zone is an important source of toughening. In this paper, both catastrophic and non-catastrophic failure modes are taken into consideration and it is shown that it can be classified from the inverse analysis results. In this regard, fiber strengths are considered to be random in a statistical point of view and assumed to fall according to a Weibull distribution of modulus μ. It is shown in [5] that the bridging stress and COD relation can be approximated by the following equation which is shown in Fig. 2 for different values of shape parameter μ.

$$p(u) = \sqrt{u}\, e^{-u^{\frac{\mu+2}{2}}} \qquad (1)$$

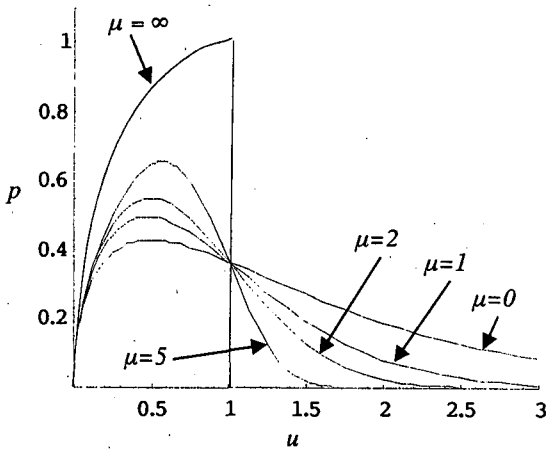

Fig. 2: Fiber bridging stresses (p) vs. pull-out distance (u) for fibers with strengths given by Weibull distribution with different values of shape parameter μ.

2. Crack analysis

Cracks in CA brittle-matrix composites can be formulated by the following equation [2]

$$u(x) = \frac{4}{E'}\int_x^a \left\{\int_0^s G(t,s,w)\{\sigma_a(t) - p[u(t)]dt\}\right\} G(x,s,w)ds \qquad (2)$$

where $2a$ is the crack length for embedded straight cracks and a is the same for single edge cracks, w is one or more specimen dimension e.g. width, $\sigma_a(x)$ is the stress that would exist on the fracture plane in the absence of the crack, E' is a combination of elastic constants, which depends on whether the crack is on plane stress or plain strain and whether the material is isotropic or orthotropic and G is a weight function which depends on the crack geometry only. Standard forms of G for a large number of crack configurations can be found in the handbooks of crack analysis e.g. [6]. However, this paper dealt with embedded straight cracks and single edge cracks in an infinite specimen for which G has the form [6]

$$G(x,a,w) = \frac{1}{\sqrt{\pi a}} \frac{h_1(x/a, a/w)}{\left(1 - x^2/a^2\right)^{1/2}} \qquad (3)$$

where $h_1(x/a, a/w) = 1$, for straight embedded cracks and $h_1(x/a, a/w)$ for single edge cracks is given in the appendix. In Eq. (2), t, s stand for coordinates along the crack.

The problem solved here is mathematical inversion of Eq. (2) for known crack configurations and known external stresses. Experimental COD data will be exploited for inverse analysis. However, as experimental data are always prone to noise, regularization technique is needed to get good analytical approximation of bridging stresses. For the present purpose, Tikhonov method of regularization [7] has been called upon to treat noisy data. Applicability of Tikhonov regularization to this type of composite bridging stress evaluation has been proven successful in [2].

3. Formulation

Numerical inversion of Eq. (2) means $p[u(x)]$ be determined when $u(x)$ is known. For this reason, $p(u)$ is, at first, expanded in a set of basis functions as

$$p(u) = \sum_{i=0}^{n} \alpha_i f_i(u) \qquad (4)$$

where n should be restricted to finite order. In this study, n=10, is found to be adequate for mathematical approximation or sometimes the difference becomes negligible after n=8. However, larger values of n lead to mathematical instability and abnormally long time for solution with standard packages. As for basis functions, Legendre polynomials have been chosen here. Once basis functions are fixed, the solution requires only finding out α's.

Let us assume that we are given with experimental data as

$$\left[\{x_j, u_j\}, j = 1, \ldots\ldots, m\right] \qquad (5)$$

with which a function $\tilde{u}(x)$ can be formed by interpolating amongst them. The collected data and interpolation should be such that errors near the crack tip are minimized. This can easily be done by taking more data points near the crack tip and interpolating the function as $f(x)\sqrt{a^2 - x^2}$. If Eq. (4) is substituted into Eq. (2) and appropriate weight functions are used from Eq. (3), we shall be left with a system

$$\mathbf{A}.\boldsymbol{\alpha} = \mathbf{b} \qquad (6)$$

Where

$$A_{ji} = \frac{4}{E'}\left\{\int_{x_j}^{a}\int_{0}^{s} G(t,s,w) f_i[u(t)]dt\right\} G(x_j,s,w)ds \quad (7)$$

$$b_j = \frac{4}{E'}\left\{\int_{x_j}^{a} G(t,s,w)\sigma_a(t)dt\right\} G(x_j,s,w)ds \quad (8)$$

If data were noiseless, it would enough to solve Eq. (6) for α's. But, as experimental data will always contain some levels of noise, Tikhonov's regularization has been employed here where one seeks to minimize the following functional

$$J_\beta = \left\|\tilde{u}(x_j) - u_j\right\|^2 + \beta\|p\|^2 \quad (9)$$

where the norms are defined in the following ways.

$$\left\|\tilde{u}(x_j) - u_j\right\|^2 = \sum_{j=1}^{m}\left\{\tilde{u}(x_j) - u_j\right\}^2 \quad (10)$$

$$\|p\| = \int_0^{\infty}\left|\frac{d^k p(u)}{du^k}\right| du \quad (11)$$

Stationary condition of (9) with respect to the variation of α's leads to the following n dimensional system

$$(\mathbf{P} + \beta\,\mathbf{T})\boldsymbol{\alpha} = \mathbf{Q} \quad (12)$$

where

$$\mathbf{P} = \mathbf{A}^{\mathrm{T}}\mathbf{A} \quad (13)$$

$$\mathbf{Q} = \mathbf{A}^{\mathrm{T}}\mathbf{b} \quad (14)$$

$\mathbf{T}$ is derived from Eq. (11) by replacing $p(u)$ from Eq. (4) and it was found that the elements of this $n \times n$ matrix are

$$T_{ij} = \int_{u_{min}}^{u_{max}} f_i f_j du \quad (15)$$

for $k = 0$. Different values of k do not largely change the results which have been checked here. The optimal choice for the parameter β is such that the correct value of β will yield the root mean square deviation of the model from the data equal to the square of experimental noise level.

4. Specimens of infinite width

4.1 Embedded straight cracks

No experiment was performed within this course of research, so synthetic data were created by forward analysis of Eq. (2) with an assumption of $p(u)$ from Eq. (1). Detailed description of the methods of forward analysis can be found in [3] and [4] where similar integral equations have been solved to determine crack opening displacements with known functions of bridging stresses. The results from forward analysis for an embedded straight crack are shown in Fig. 3 for different external stress levels, normalized as $S = \sigma_\infty / f\Sigma$, where f is the volume fraction of ductile fiber in the composite and Σ is a parameter related to the average stress in the fibers when they break.

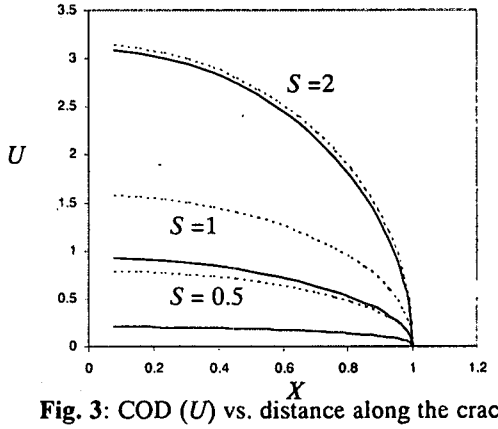

Fig. 3: COD (U) vs. distance along the crack (X) for an embedded straight crack in an infinite width specimen. The solid curves show the self-consistent forward analysis solutions after a sufficient number of iterations where the dashed curves show the profile that would exist in absence of bridging.

In Fig. 3, crack opening displacements have been normalized as $U = u/u_n$ with

$$u_n = \frac{\Sigma^2 R(1-f)E_m}{4\tau E_f E} \quad (16)$$

where R is the radius of the fiber, E_m, E_f are the Young's moduli of the matrix and the fiber, E is the same for composite and τ the interfacial shear strength between the matrix and the fiber. Distance along the crack has been normalized as $X = x/a$.

Data points were collected from Fig. 3 to use as input into inverse analysis. Random numbers, created with Gaussian distribution of zero mean and ω width are added to these data to simulate practical noisy situation. Inverse analysis was performed on these noisy data by minimizing the Tikhonov's functional in Eq. (9). The results from inverse analyses for the uppermost solid line in Fig. 3 are shown in Fig. 4a for different levels of simulated noise indicated in the figure. Here C stands for normalized crack length as $C = a / c_n$

$$\text{where } c_n = \frac{\pi \Sigma R (1-f) E_m}{16 \pi f E_f (1-\nu^2)} \qquad (17)$$

Compared with Fig. 2 it is noticed that the tail of the curve is retrieved with acceptable accuracy whereas the rising limb has been retrieved poorly. For this reason, this portion has been evaluated independently in Fig. 4b for load parameter S=1 and same geometry where bridging stress boundary is up to COD parameter 0.8. It is noticed that higher noise levels lose accuracy. So it is recommended to reduce experimental noise level as much as possible.

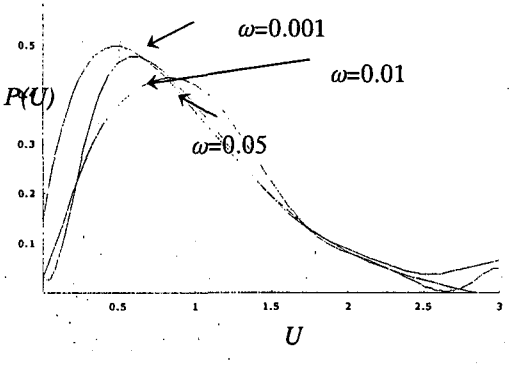

Fig. 4a: Comparison of estimates of crack bridging stresses with different levels of noise width ω = 0.001, 0.01, 0.05 for S=2 and C=1 for embedded cracks in a specimen of infinite width.

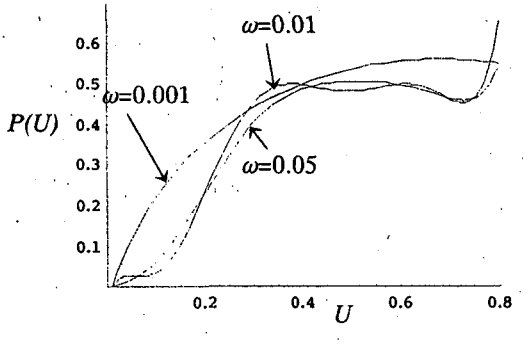

Fig. 4b: Comparison of estimates of crack bridging stresses with different levels of noise width ω = 0.001, 0.01, 0.05 for S=1 and C=1 for embedded cracks in a specimen of infinite width.

4.2 Single edge cracks

Analyses for a single edge cracked specimen of infinite width under uniform tensile stresses are almost identical to those of embedded cracks solved earlier. Only different weight function given is the appendix is needed to use in the integral equation with $a / w \to 0$ for infinite width. Forward analyses results for this case are shown in Fig. 5 for different external load levels.

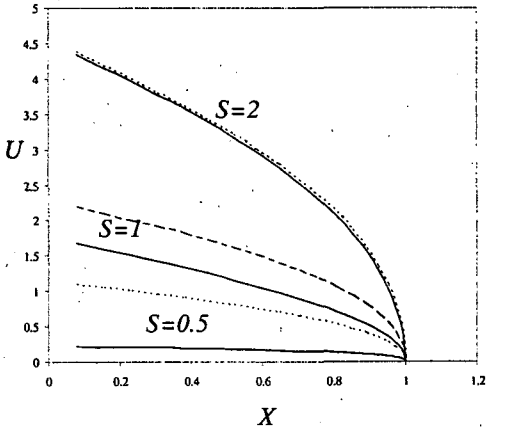

Fig. 5: COD (U) vs. distance along the crack (X) for single edge cracked specimens of infinite width. The solid curves show the self-consistent forward analysis solutions where the dashed curves show the profile that would exist in absence of bridging.

Data points, collected from Fig. 5, have been made noisy in a similar way. The inverse analyses results for external load parameter S=2 are shown in Fig. 6a and for S = 1 in Fig. 6b to get better estimation of the rising part before peak.

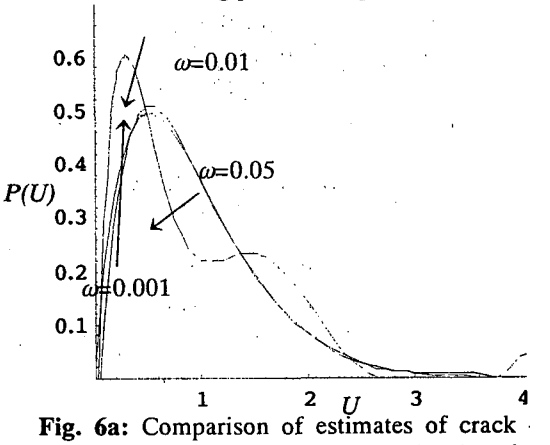

Fig. 6a: Comparison of estimates of crack bridging stresses with different levels of noise width ω = 0.001, 0.01, 0.05 for S=2 and C=1 for single edge cracks in a specimen of infinite width.

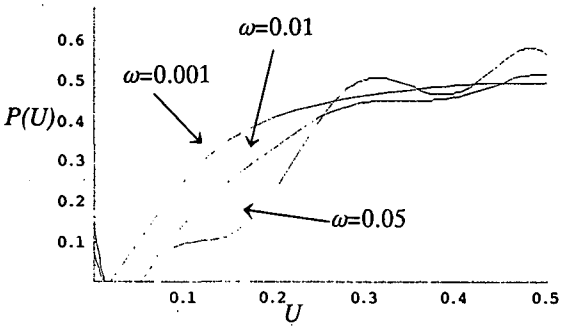

Fig. 6b: Comparison of estimates of crack bridging stresses with different levels of noise width ω = 0.001, 0.01, 0.05 for S=1 and C=1 for single edge cracks in a specimen of infinite width

5. Specimens of finite width

Single edge cracked specimens of finite width under bending stresses are of practical interest from a civil engineering point of view. Such a specimen under bending stress at the edges of width w with a crack at the middle on its bottom face is shown in Fig. 7, which practically can be either under pure bending or under four-point loading. Modeling of such specimen is also possible with similar integral equation and similar procedure can be followed to solve forward and inverse problems described in the previous sections. The only difference will be in the applied tensile stresses which is now a function of the distance along the crack. This specimen can also be modeled with the same weight functions for single edge cracked specimen given in the appendix, with the exception that it will be a function of crack length (a), distance along the crack (x) and specimen width (w) as well. However, this weight function and linear distribution of stresses along the edges of the specimen make the integration scheme more complicated and time consuming.

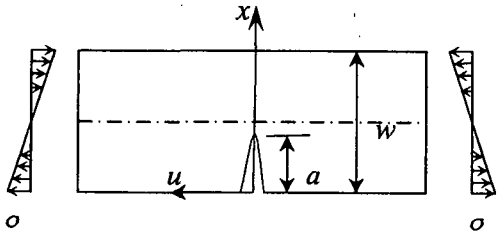

Fig. 7: Single edge cracked specimen of finite width w acted upon by bending stresses at the edges.

In a similar way, synthetic data were created by solving the forward problem to perform inverse analysis. Data were made noisy as usual. The results of the inverse analyses are shown in Fig. 8a and Fig. 8b. The profile of Eq. (1) is retrieved satisfactorily again.

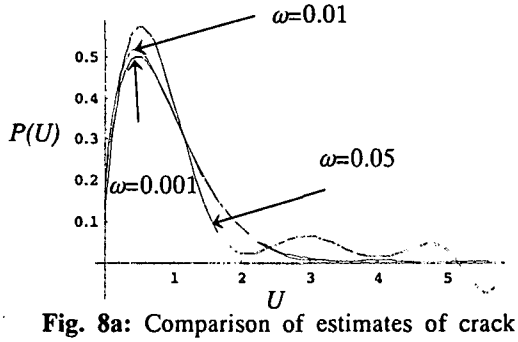

Fig. 8a: Comparison of estimates of crack bridging stresses with different levels of noise width ω = 0.001, 0.01, 0.05 for S=2 and C=1 for single edge cracks in a specimen of finite width under bending stresses.

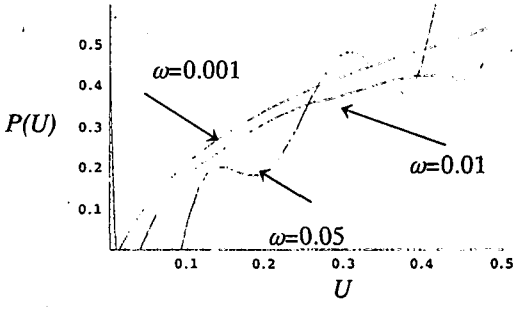

Fig. 8b: Comparison of estimates of crack bridging stresses with different levels of noise width ω = 0.001, 0.01, 0.05 for S=1 and C=1 for single edge cracks in a specimen of finite width under bending stresses.

6. Fully bridged and partially bridged cracks

One of the interesting features of the inverse analysis is that one can perform the same procedure to determine bridging stress as a function of the distance along the crack (x) in Fig. 7. To do this, one has just to expand the bridging stress with the basis functions (Legendre polynomials in Eq. (4) as functions of distance along the crack. If bridging stresses are supposed to be discontinuous like what in reinforced concrete or fiber composites with discrete bridging ligaments, $f_i(x)$ can be chosen as a piecewise constant or piecewise linear approximation. Inverse analysis can be performed in a same way. The results of such analyses are shown in Fig. 9a for single edge cracked specimen

under tensile stress and in Fig. 9b for the same specimen under bending stresses but under different magnitude of load level.

It is clearly noticed in Fig. 9b that bridging is significant only near the crack tip and almost equal to zero elsewhere, which indicates that this crack is partially bridged. These types of cracks propagate in a catastrophic way with fibers broken in most parts of the crack only except a small portion behind the crack tip. But, this situation generally does not occur at service condition for most of structures. Structural damage is initiated with the failure of brittle matrix with cracks propagating in a fully bridged situation in which case, the variations of bridging stresses along the distance of the crack are shown Fig. 9a. It is clearly noticed that bridging is more or less uniform along the entire crack length and significant everywhere, which obviously indicates a fully bridged situation. So, it can be concluded from these analyses that catastrophic and non-catastrophic failure modes can be easily characterized if inverse analysis is done on the crack opening profile with applied stress. Using fully-bridged cracks' solutions for structures in service, allowable service load can be determined.

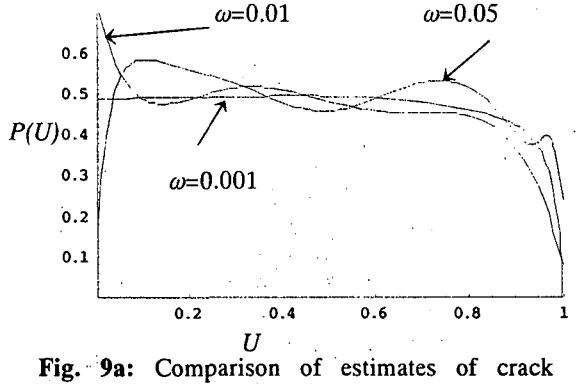

Fig. 9a: Comparison of estimates of crack bridging stresses ($P(U)$) along the distance of the crack (X) with different levels of noise width ω = 0.001, 0.01, 0.05 for S=0.75 and C=1 for fully-bridged, single edge cracked specimen of infinite width under tensile stress.

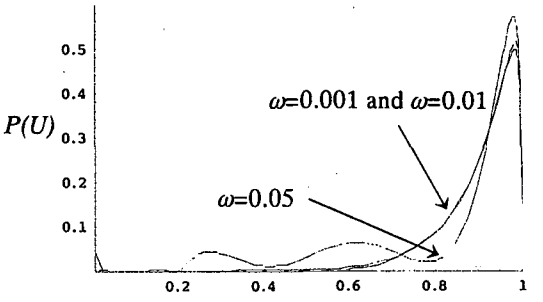

Fig. 9b: Comparison of estimates of crack bridging stresses ($P(U)$) along distance of the crack (X) for different levels of noise width ω = 0.001, 0.01, 0.05 for S=2 and C=1 for partially-bridged, single edge cracks of finite width specimen under bending stress.

7. Data from several fully bridged cracks

It has been noticed in the inverse analyses solutions that the bridging profiles become more and more approximate if the noise level increases. So, it may be quite difficult to get exact bridging law with practical COD data. However, data from several cracks can be utilized to minimize the errors from individual crack profiles. Several cracks under different stresses can be analyzed simultaneously to get the bridging stresses with respect to crack opening displacements. Cracks under different magnitude of stresses should not generally be of same length, so different lengths are used under different loadings. The relation between crack lengths with different loadings has been demonstrated in [3]. In this study, an embedded crack under uniform remote tensile stress was analyzed with external load parameters S =1, 0.75 and 0.5 with crack length parameter C = 1, 0.9 and 0.4. The results are shown in Fig. 10 for different noise levels. It is found that the bridging profile is quite improved with such analyses. In Fig. 10, only the rising limb is shown for two reasons. Firstly, it was found in single crack analysis that falling limb can be more accurately retrieved than the rising limb and secondly, we are interested about the rising portion of bridging law where the cracks sustain fully-bridged conditions because, the ultimate goal of the current project is to work on existing structures which does not generally go through catastrophic failures.

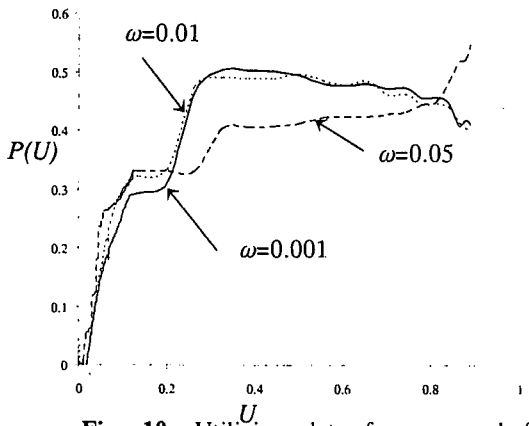

Fig. 10: Utilizing data from several fully bridged cracks of S = 1, 0.75 and 0.5 with different levels of noise width ω = 0.001, 0.01, 0.05 for an embedded crack specimen under uniform tensile stress.

8. Conclusions

Inverse analyses have been performed on COD data to get bridging laws of brittle-matrix composites. The same procedure has been successfully followed to get variation of crack bridging stresses with distance along the crack. If collected data are within sufficient levels of noise, the accurate bridging profile can be estimated with the procedure described in this paper. However, estimating bridging stress for small COD is quite difficult as the rising portion of the retrieved bridging law is more sensitive than the other part. Again, measuring COD near the crack tip is complicated task from an experimental point of view. So, data from several cracks with different cracks lengths and different applied loads should be utilized to get bridging stresses for those values of COD. It is proven in this paper that this method works very well for embedded cracks and single edge cracks with tensile and bending stresses. However, it should work identically for other cases, e.g. double edge cracked and compact tension specimens with finite or infinite width and under tensile or bending stresses.

REFERENCES

1) Matsumoto, T.: *Fracture Mechanics Approach to Fatigue Life of Discontinuous Fiber Reinforced Composites*, PhD thesis, The University of Michigan, 1998.
2) Cox, B.N. and Marshall, D.B.: The determination of crack bridging forces, *I. J. of Frac.* Vol.**49**, pp. 159-176, 1991.
3) Cox, B.N. and Marshall, D.B.: Stable and unstable solutions for bridged cracks in various specimens, *Acta Metall. Mater.*, Vol.**39**, No.**4**, pp. 579-589, 1991.
4) Marshall, D. B., Cox, B.N. and Evans, A.G.: The mechanics of matrix cracking in brittle-matrix fiber composites, *Acta Metall.*, Vol.**33**, No.**11**, pp.2013-2021, 1985.
5) Cox, B.N., Marshall, D. B. and Thoules, M.D.: Influence of statistical fiber strength distribution on matrix cracking in fiber composites, *Acta Metall.*, Vol.**37**, No.7, pp.1933-1943, 1985.
6) Tada, H.: *The Stress Analysis of Cracks Handbook*, 2nd Ed., Paris Productions, Inc., St. Louis, Missouri, 1985.
7) Kirsch, A.: *An Introduction to the Mathematical Theory of Inverse Problems*, Springer-Verlag New York, Inc., 1996.
8) Kitsutaka, Y.: Fracture parameters by polylinear tension-softening analysis, *J. of Engrg. Mech.*, Vol.**123**, No.**5**, pp. 444-450, 1997.

Appendix

Weight function for single edged cracked specimen is expressed with the help of following $h_1(x/a, a/w)$ function as

$$h_1(x/a, a/w) = \frac{g(x/a, a/w)}{(1-a/w)^{3/2}} \quad \text{(A-1)}$$

where $g(x/a, a/w) = g(r,s)$ is given by

$$g(r,s) = g_1(s) + rg_2(s) + r^2 g_3(s) + r^3 g_4(s) \quad \text{(A-2)}$$

$$g_1(s) = 0.46 + 3.06s + 0.84(1-s)^5 + 0.66s^2(1-s)^2 \quad \text{(A-3)}$$

$$g_2(s) = -3.52s^2 \quad \text{(A-4)}$$

$$g_3(s) = 6.17 - 28.22s + 34.54s^2 - 14.39s^3 - (1-s)^{3/2} - 5.88(1-s)^5 - 2.64s^2(1-s)^2 \quad \text{(A-5)}$$

$$g_4(s) = -6.63 + 25.16s - 31.04s^2 + 14.41s^3 + 2(1-s)^{3/2} - 5.04(1-s)^5 + 1.98s^2(1-s)^2 \quad \text{(A-6)}$$

(Received April 18,2003)